Atmospheric Pollution Research 13 (2022) 101313

Contents lists available at ScienceDirect

Atmospheric Pollution Research

journal homepage: www.elsevier.com/locate/apr

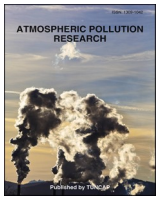

Influence of conducive weather on ozone in the presence of reduced NO_x emissions: A case study in Chicago during the 2020 lockdowns

Ping Jing [a,*], Daniel L. Goldberg [b]

[a] Loyola University Chicago, School of Environmental Sustainability, Chicago, IL, USA
[b] Department of Environmental and Occupational Health, George Washington University, Washington, DC, USA

ARTICLE INFO

Keywords:
Ozone
NO_x
Air quality
COVID-19
Chicago

ABSTRACT

This study analyzes the response of near-surface O_3 in Chicago to the COVID-19 lockdowns using observational data at the surface and from satellite. Even though the lockdowns caused NO_x emissions to decrease by 18%, Chicago still experienced 17 high-O_3 (>70 ppb) days in 2020, and the mean O_3 mixing ratio did not show a significant change in 2020 compared with 2015–2019. Ozone production in summer 2020 in Chicago was in the "transitional" regime ($HCHO/NO_2$ column ratio = 2.9), and not sensitive to changes in NO_x in either direction. The primary driver for Chicago's O_3 exceedances in 2020 was the dry tropical (DT) weather, which was associated with hot, dry, and stagnant meteorological conditions. There were 15 DT days in 2020, which led to more efficient production and greater accumulation of O_3. The results suggest that a dramatic one-year 18% NO_x reduction can be overcome by conducive meteorology and that NO_x and VOC controls need to be more substantial and wide-ranging. This study also highlights the important role of different climate regimes, and not solely temperature, on the formation of O_3.

1. Introduction

Despite strenuous efforts over the past 30 years to reduce ozone (O_3) concentrations, large areas of the U.S. continue to experience elevated O_3 concentrations in summertime; and many cities, including Chicago, are still listed as Nonattainment Areas for the O_3 National Ambient Air Quality Standard by the U.S. Environmental Protection Agency (EPA) (U.S. EPA, 2021). Over five million people in Chicago are at risk from elevated levels of O_3 and particle pollution (American Lung Association, 2019). This means that O_3 pollution is still a great concern for public health for cities in the U.S., including Chicago. It's important to study O_3 not only because it has adverse effects on human health and ecosystems but also because it plays a central role in photochemical reactions that determine the lifetime of other air pollutants. Ozone forms by the complex nonlinear photochemical reactions of nitrogen oxides (NO_x) and volatile organic compounds (VOC) (Sillman, 1995). In general, O_3 concentrations increase when both NO_x and VOC increase. In conditions where the VOC/NO_x ratio is high, peroxide radicals' reactions with themselves (instead of with NO_x) dominate the radical sink, and O_3 production has a linear relationship with NO_x but independent of VOC (Jacob, 1999). This case is referred to as the "NO_x-limited regime" because O_3 production is limited by the amount of NO_x. In conditions where the VOC/NO_x ratio is low, the dominant sink for peroxide radicals is the reaction of NO_2 with OH to form nitric acid. Ozone production increases linearly with increasing VOC concentration but inversely with NO_x (Jacob, 1999). This case is called the "VOC-limited regime" because O_3 is lowered by reducing VOC. In between the two regimes is an ambiguous "transition regime" in which O_3 production is sensitive to reductions in both NO_x and VOC (Schroeder et al., 2017). Summertime O_3 production in the Chicago area generally transitioned from VOC-limited in 1996–2000 toward NO_x-limited in 2013–2016 (Jin et al., 2020). Understanding the O_3-NO_x-VOC relationship is important not only for atmospheric science but also for developing efficient and effective public policy.

The COVID-19 lockdowns resulted in reduced fossil-fuel burning activities worldwide, and therefore global NO_x emissions dropped by 30% in April 2020 (Forster et al., 2020). Based on the NO_2 vertical column density values measured by the Tropospheric Monitoring Instrument (TROPOMI), 10–70% reductions of NO_2 occurred in most urban areas worldwide in March–June 2020 compared with the same

Peer review under responsibility of Turkish National Committee for Air Pollution Research and Control.
* Corresponding author.
E-mail address: pjing@luc.edu (P. Jing).

https://doi.org/10.1016/j.apr.2021.101313
Received 30 September 2021; Received in revised form 13 December 2021; Accepted 31 December 2021
Available online 4 January 2022

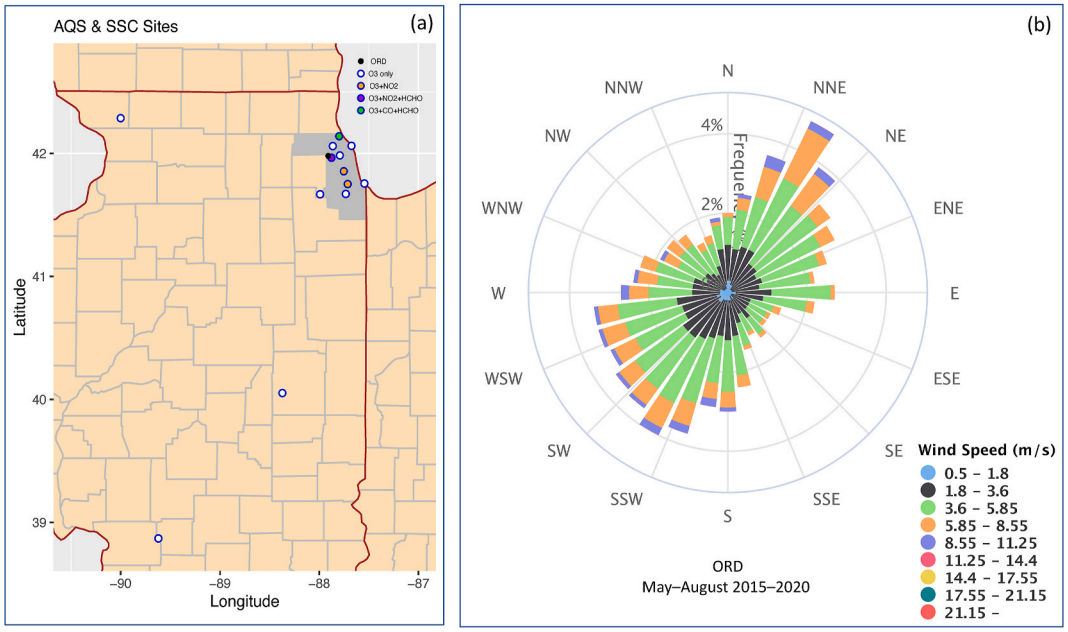

Fig. 1. (a) Locations of the ORD airport that measures weather conditions and the AQS sites that provide air pollution data. The gray shaded area shows Cook County, Illinois, where the City of Chicago is located. The AQS sites located in the gray area are considered to be "urban" and the three sites outside are "rural". (b) Wind rose that shows the average May–August wind conditions at ORD between 2015 and 2020. The radical scale denotes the frequency of counts by wind direction sector.

period in 2019, and the urban NO_2 reductions were correlated with reduced traffic activities (Bauwens et al. et al., 2020; Goldberg et al., 2020). The reduction of NO_x emissions due to COVID-19 provides a unique opportunity to investigate the sensitivity of O_3 concentrations to NO_x emissions. Global free tropospheric O_3 decreased in spring and summer 2020 in response to global NO_x emissions reductions (Miyazaki et al., 2021; Steinbrecht et al., 2021). Modeling results for mid-March to mid-April 2020, a timeframe with climatologically low O_3 concentrations in the northern extratropics, show that emissions reductions due to the lockdowns led to a slight increase (2%–10%) in surface O_3 concentrations in urban areas of the Midwestern and Northeastern U.S. (Gaubert et al., 2021). A few other studies have investigated the effects of NO_x emission reduction on O_3 in different regions of the world by analyzing observations (Brancher, 2021; Cazorla et al., 2021; He et al., 2021; Naqvi et al., 2021; Sokhi et al., 2021) and through photochemical model simulations (Soni et al., 2021). The results of these studies have shown heterogeneous responses of O_3 to NO_x reductions. Because of the non-linear relationship between O_3 and NO_x, if VOC decreases were slower than NO_x reductions, O_3 concentrations could increase in VOC-limited conditions (Brancher 2021; Soni et al., 2021). The purpose of this paper is to find out if ground-level O_3 in Chicago experienced a reduction in the summer of 2020, the peak of the climatological O_3 season. Chicago in Illinois is the most populated city in the Midwestern U.S. The Stay-at-Home Executive Order issued by the Governor of Illinois was effective from 1 May to May 30, 2020. Prior to that, schools, universities, bars and restaurants in Illinois were closed in mid-March 2020. All schools stayed closed, and the economic activities remained low for the rest of 2020. Studying its O_3 response to emission changes due to COVID-19 lockdowns could provide insight into the formation of air pollution in similar urban areas.

It is well known that weather conditions also affect ground-level O_3 concentrations. There is a positive correlation between O_3 and temperature (Camalier et al., 2007; Bloomer et al., 2009). Ozone concentrations are also controlled by wind speed and direction (Kerr et al., 2019). Weather conditions that produce warm temperatures are associated with clear-sky and stagnant air, which contributes to more efficient photochemical production and greater accumulation of O_3. Furthermore, there are greater biogenic VOC emissions with increasing temperatures in the presence of non-drought conditions (Guenther et al., 2006). Studies have shown that elevated O_3 concentrations are associated with increased temperatures, reduced cloud fraction, and increased air stagnation (Jing et al., 2014, 2017; Jaffe and Zhang, 2017). Therefore, this study will also consider the effect of meteorological conditions on O_3 in Chicago.

2. Methods

This study analyzes the summertime O_3–NO_2 relationship in the Chicago region in 2020 and compares it to the pre-COVID-19 period from 2015 to 2019. The pre-pandemic period is defined as 2015–2019 so that it is long enough to avoid the influence of year-to-year changes in weather conditions and short enough to not include the longer-term trends of O_3 and NO_2 in 1990–2015 that have been previously studied (e.g., Jing et al., 2017). This study focuses on the summer season (May to August), because that is when the elevated O_3 concentration events are most likely to occur. This period also coincided with the official Stay-at-Home Executive Order mandated by the Governor of Illinois, which became effective on May 1, 2020.

2.1. Ground monitor data

Air pollutant data, including daily maximum 8-h O_3, daily maximum 1-h NO_2, daily maximum 8-h carbon monoxide (CO), and daily mean formaldehyde (HCHO) mixing ratios are obtained from U.S. EPA Air Data archives. This study focuses on the city of Chicago, which is defined as the area between 41.65°N and 42.15°N latitude, and between 87.5°W and 88.0°W longitude (Fig. 1). It encompasses all the non-rural monitoring stations around Chicago in the U.S. EPA's Air Quality System (AQS). To minimize the influence of missing data, we require each station to have summertime observations that cover the entire 2015–2020 period. Ten AQS stations (site codes 17-031-0001, 17-031-0032, 17-031-0076, 17-031-1003, 17-031-1601, 17-031-3103, 17-031-4002, 17-031-4007, 17-031-4201, and 17-031-7002) meet this criterion for O_3 observations, among which three stations (17-031-0076, 17-031-3103,

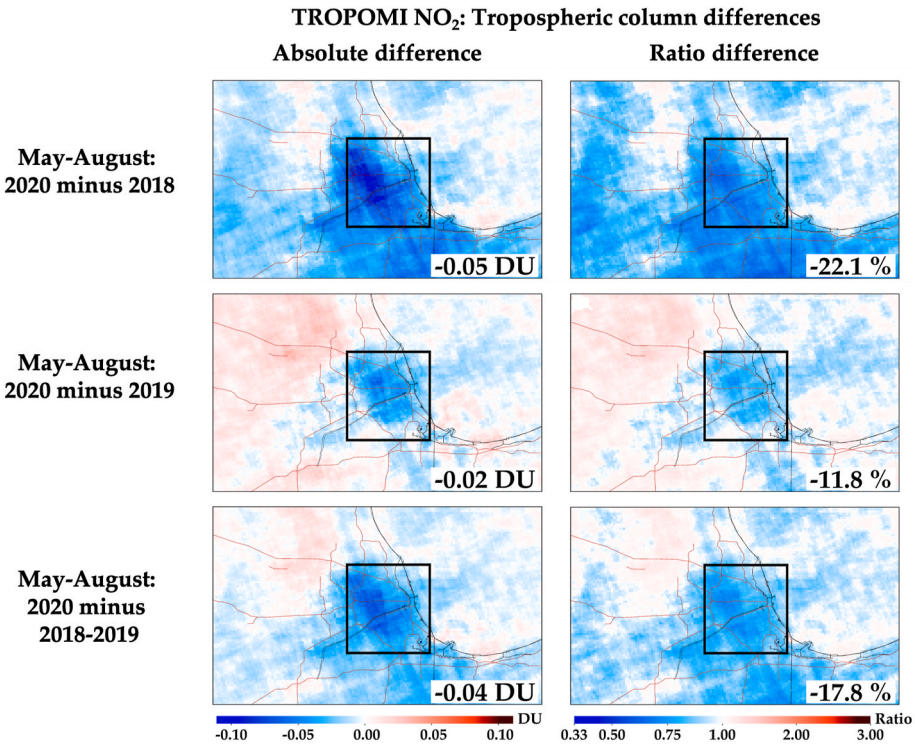

Fig. 2. TROPOMI NO_2 changes around Chicago in May–August 2020 compared with the same period in 2018, 2019, and 2018–2019. Plots show the differences in Dobson units (DU) and the ratio between years. The black box includes Chicago and the closest suburbs, and the mean value of NO_2 changes inside the box is provided on the lower right corner of each plot.

and 17-031-4002) also meet the criterion for NO_2 observations, and one (17-031-4201) also meets the criterion for CO. Two stations (17-031-3103 and 17-031-4201) also provide HCHO observations. While O_3, NO_2, and CO have daily observations, HCHO is typically measured once every six days. We have analyzed the correlation of temporal variability among O_3 concentrations at the different sites as well as the spatial homogeneity of the O_3 data among sites, using the methods of Yadav and Turner (2014) and Wilson et al. (2005). The results show that O_3 concentrations observed at the sites are homogeneous, which is consistent with the regional nature of O_3 formation, and that observations at each site are representative of the Chicago area. This study also considers three rural sites (17-085-9991, 17-019-1001, and 17-119-9991) in the Clean Air Status and Trends Network (CASTNET) of the U.S. EPA. They are located to the west and southwest of Chicago. Because the prevailing winds come from the southwest direction during summer, we can use O_3 measurements at these three rural sites to represent upwind "background" O_3 levels outside of Chicago.

Because O_3 is a regional pollutant, not directly tied to point sources of emissions, this study examines how O_3 concentrations are influenced by regional-scale weather phenomena (as distinct from local-scale meteorological conditions). To analyze the relationship between O_3 and synoptic weather conditions, this study employs the results of the Spatial Synoptic Classification (SSC) (Sheridan, 2002). Using surface-based observations of temperature, dew point, cloud cover, sea-level pressure, and south-north and west-east wind components, the SSC method classifies the weather at a given location on a daily basis into one of six types (i.e., dry moderate, dry polar, dry tropical, moist moderate, moist polar, and moist tropical), or as a transition between two weather types. In a sense, the SSC method develops a weather "calendar" for a given location. The results are available for 327 stations in North America with an average length of 50 years. This study uses the SSC data for the station at O'Hare International Airport (ORD; shown as the black dot in Fig. 1a) for the period 2015–2020 to represent the synoptic weather conditions in the Chicago area. This study also uses the daily observed air temperature and precipitation data from the Midwestern Regional Climate Center for the station at O'Hare. This study also uses the daily observed air temperature and precipitation data from the Midwestern Regional Climate Center for the station at O'Hare.

2.2. Satellite data

TROPOMI observations of tropospheric column NO_2 were used to document the spatial changes of NO_2 pollution in the Chicago area. TROPOMI is a polar-orbiting satellite instrument measuring NO_2 column densities during the early afternoon (~13:30 local time) with daily or twice-daily coverage in the Chicago area at a spatial resolution of 3.5 $\times$ 7 km^2 (3.5 $\times$ 5.5 km^2 starting August 2019). Satellite data are filtered to use only the highest quality pixel measurements (qa_value $>$ 0.75); this filter automatically screens for high cloud fractions ($>$0.5) and other problematic features that cause erroneous measurements. We use observations from the coincident timeframe with the ground monitors (May–August). TROPOMI measurements are only available starting in 2018, so we compare 2020 data to 2018 and 2019 data only. We use the version 1 TROPOMI NO_2 algorithm with appropriate sub-versions for each timeframe. We also examine changes in tropospheric column O_3 using the monthly-mean tropospheric column O_3 at a spatial resolution of 1.25° longitude by 1° latitude that is determined using the residual method between the total column O_3 from the Ozone Monitoring Instrument (OMI) and stratospheric O_3 from the Microwave Limb Sounder (MLS) (Ziemke et al., 2006).

3. Results

3.1. O_3 in 2020 compared with the pre-pandemic period

COVID-19 lockdowns resulted in lower NO_x emissions worldwide and caused tropospheric O_3 to decrease by 15% globally and by as much as 50% locally by June 2020 (Miyazaki et al., 2021). According to

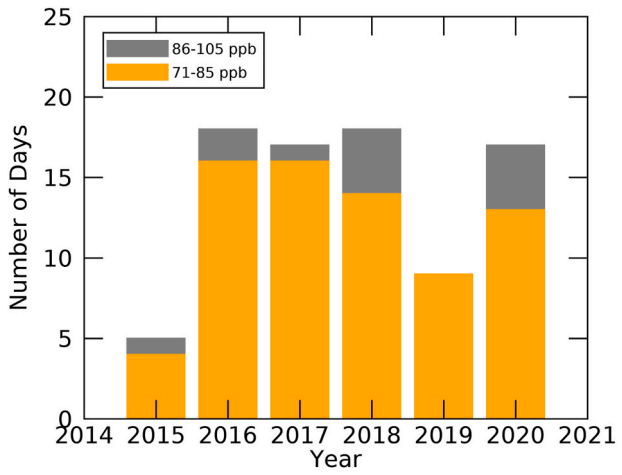

Fig. 3. Number of days when Chicago's daily maximum 8-h O_3 concentrations exceeded 70 ppb in 2015–2020.

TROPOMI observations, around Chicago the tropospheric NO_2 in May–August 2020 decreased by an average of 17.8% compared with the same period in 2018–2019 (Fig. 2), consistent with reduced traffic and therefore reduced anthropogenic sources of NO_x.

Analysis of daily maximum 8-h O_3 mixing ratios observed at the ten AQS sites in Chicago shows that O_3 exceedances did not decrease in 2020 compared with 2015–2019 (Fig. 3). In 2020 there were 17 high-O_3 days ($O_3 > 70$ ppb), among which there were four days when O_3 levels exceeded 85 ppb. They were similar to the numbers of high-O_3 days in 2016–2018, which ranged between 17 and 18 days. These results indicate that summertime O_3 pollution in Chicago during the COVID-19 pandemic did not improve as would have been expected from the NO_x emission reductions.

3.2. O_3-related chemical species

A clearer view of the trend in O_3 concentrations in Chicago can be obtained by analyzing the mean values of the maximum daily 8-h average O_3 mixing ratio from the 10 AQS sites for each summer in 2015–2020. The mean summertime O_3 among the 10 sites shows that there was a statistically insignificant increase of 0.40 ± 0.42 ppb/yr (R^2 = 0.18) in 2015–2020, and that the mean O_3 value in 2020 remained similar to the values in 2017 and 2018 (Fig. 4a). We also examined the tropospheric column O_3 in the Chicago area using the monthly-mean tropospheric column O_3 derived from OMI/MLS satellite observations (Ziemke et al., 2006), and the results show that although summertime mean tropospheric column O_3 increased by 3 DU in 2020 compared with 2019, it was at the similar level as those in 2015–2018 (Fig. 4b).

Analysis of daily maximum 1-h NO_2 mixing ratios at the three AQS NO_2 sites shows that the mean summertime NO_2 decreased by 0.54 ± 0.49 ppb/yr (R^2 = 0.23) in 2015–2020 (Fig. 4c). These results demonstrate that the overall decrease of ground-level NO_2 between 2015 and 2020 was not accompanied by a decrease of O_3. More specifically, the O_3 concentration in 2020 increased by 5% in the median and 9% in the 95th percentile compared with 2019, while ground-level NO_2 concentrations remained unchanged. This is seemingly contradictory to the observed changes in TROPOMI column NO_2, which decreased by 11.8% in 2020 from 2019 in the Chicago area (Fig. 2). The disagreement between TROPOMI and the ground monitors is probably due to the temporal mismatch between the 1-h maximum ground monitor value and satellite observation time. The ground monitors report the 1-h maximum value, which is typically recorded in the early morning; this value is highly dependent on the early morning meteorology and boundary layer height. TROPOMI observes NO_2 pollution in the early afternoon around 13:45 local time. One might expect that in the presence of reduced NO_x emissions the 1-h maximum should have also dropped; this implies that meteorology was the cause for the flat trend in the ground monitors, since it has been well documented that NO_x emissions in 2020 dropped regionally (Harkins et al., 2021).

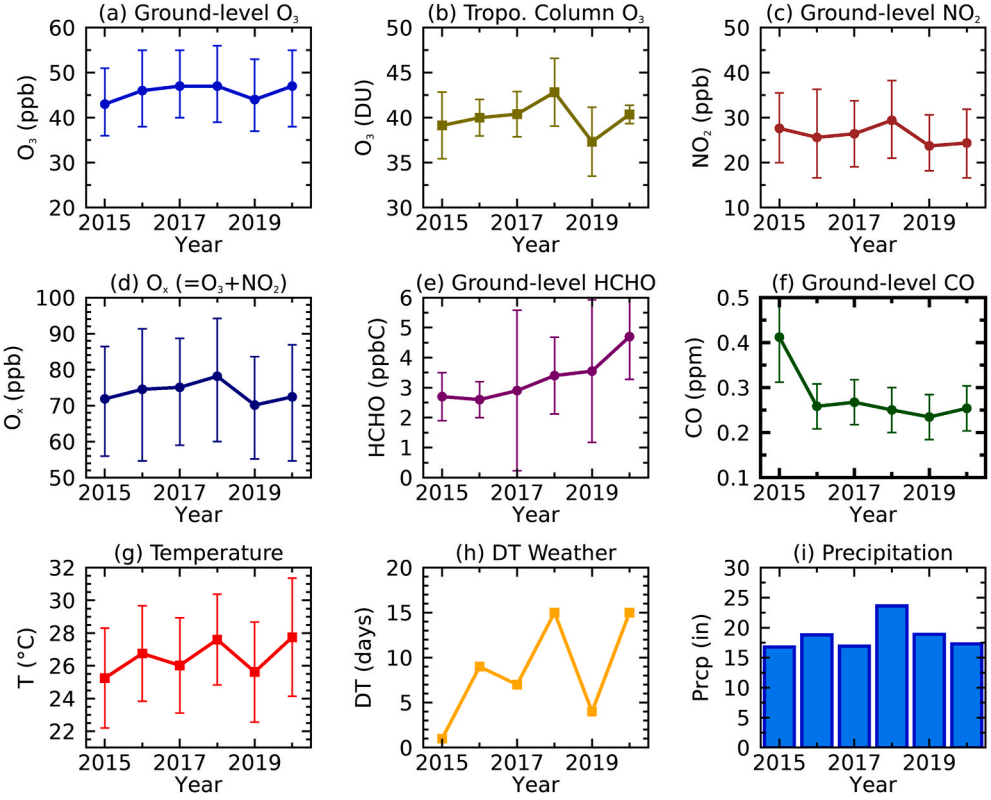

Fig. 4. Chicago's summertime (a) mean daily maximum 8-h ground-level O_3, (b) mean monthly average tropospheric column O_3, (c) mean daily maximum 1-h ground-levelNO_2, (d) mean ground-level O_x, (e) mean daily average ground-level HCHO, (f) mean daily maximum 1-h ground-level CO, (g) mean daily maximum surface air temperature, (h) total number of dry tropical weather days, and (i) total precipitation in 2015–2020. The error bars are the one-standard-deviations from the respective mean values, representing variations of data in time among the summer months of each year.

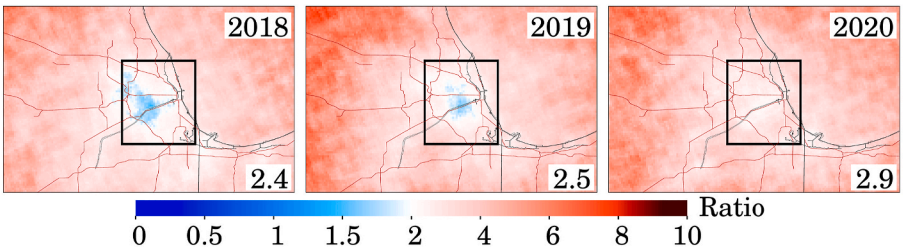

Fig. 5. Ratio of the summertime TROPOMI tropospheric column concentrations of HCHO/NO_2 in 2018, 2019, and 2020, respectively. The mean ratio of the Chicago area is provided on the lower right corner of each plot.

We also need to examine the potential impact of VOC, another important O_3 precursor. Formaldehyde (HCHO) is a major oxidation product of many VOC species, and it is a VOC that is linked to O_3 formation. Elevated HCHO concentrations usually indicate the presence of VOC from both biogenic and anthropogenic sources (De Smedt et al., 2015). Satellite-observed tropospheric column HCHO decreased in January–April 2020 compared with the same period in 2019 in regions that experienced reduced anthropogenic NO_x and VOC emissions (Sun et al., 2021). Surface measurements of summertime HCHO in Chicago show a 25% increase in 2020 compared with the same period in 2019, and the surface HCHO increased at 0.4 ± 0.14 ppbC/yr ($R^2 = 0.67$) in 2015–2020 (Fig. 4e). The observed surface HCHO increase in Chicago may be caused by the warmer temperatures that increased the natural sources of VOCs (Guenther et al., 2006; Zhu et al., 2014), even though transportation-related emissions of VOCs decreased in 2020. Other sources from volatile chemical products constitute half of fossil-fuel VOC emissions in industrialized cities (McDonald et al., 2018). The increased use of cleaning agents and personal care products due to COVID-19 may have caused the non-transportation VOC emissions to increase. The mean summertime TROPOMI tropospheric column HCHO in Chicago also showed a 1% increase in 2020 from 2019 (Figure S1). It is possible that total anthropogenic VOC emissions in Chicago increased in summer 2020, but further investigation is needed. Therefore, despite the continued decrease in NO_x, it is possible that higher biogenic VOC emissions enhanced the photochemical production of O_3 in some areas of the city that remain VOC-limited and thus contributed to the increase of O_3 in 2020.

We then used the ratio of TROPOMI tropospheric column concentrations of HCHO and NO_2 (HCHO/NO_2) from 2018 to 2020 to study the sensitivity of O_3 production to NO_x and VOC emissions (Fig. 5). It is generally agreed that tropospheric column HCHO/NO_2 ratios below 1 are associated with NO_x-limited conditions and ratios above 4 with VOC-limited conditions (e.g., Martin et al., 2004; Duncan et al., 2010; Shroeder et al., 2017; Jin et al., 2017). In between 1 and 4, is the "transitional" regime in which O_3 production is not affected by NOx or VOC reductions. For Chicago, Jin et al. (2020) demonstrates that values in the range of 3.2–4.1 represent a "transitional" regime. Our calculations of TROPOMI HCHO/NO_2 in the Chicago area show that the mean ratio slightly increased from 2.4 in 2018 to 2.9 in 2020. Our results therefore suggest that O_3 in Chicago in 2020 was in a transition regime, and O_3 would only decrease in the presence of both NO_x and VOC emission reductions. TROPOMI passes over the Chicago area around 13:30 local time, when the local O_3 concentration is about to reach the daily maximum. Jin et al. (2020) analyzed the probability of O3 exceeding 70 ppb given the TROPOMI HCHO/NO_2 ratio at 13:30 local time. Their results showed a nonlinear relationship between the high-O_3 probability and satellite-based HCHO/NO_2 ratio. Therefore, although our TROPOMI HCHO/NO_2 ratio cannot fully represent O_3 sensitivity throughout a day, it is sufficient to study O_3 sensitivity for high-O_3 episodes.

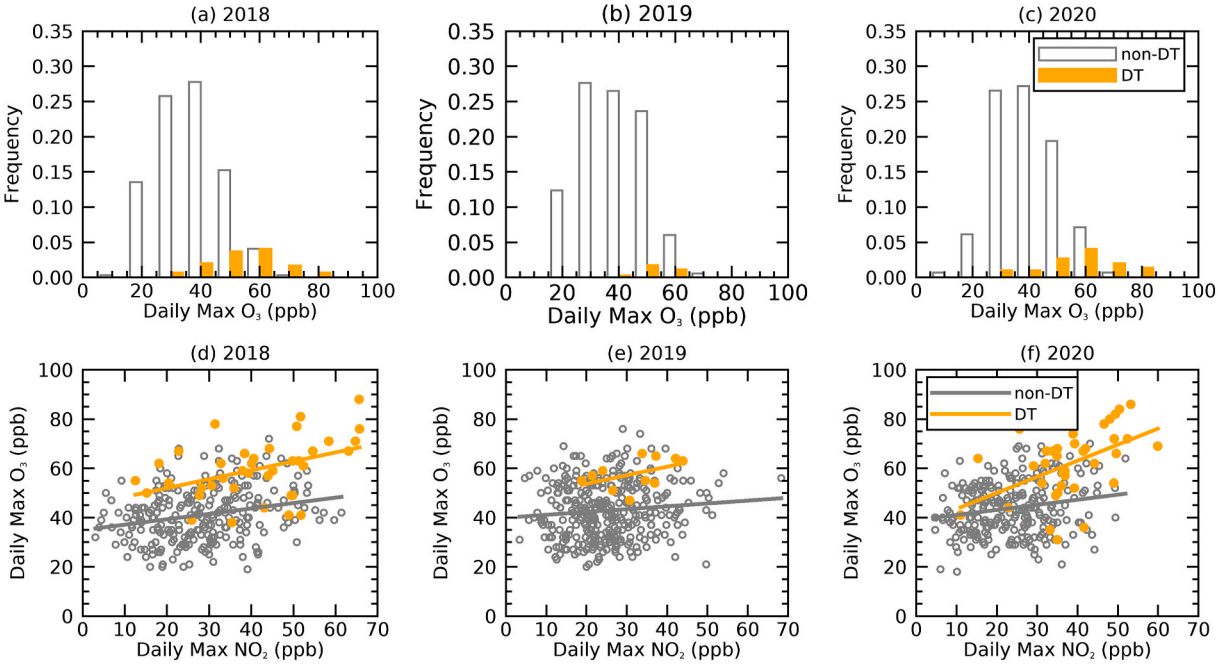

Fig. 6. (a–c) Frequency of daily maximum O_3 in DT and non-DT weather in summer months of 2018, 2019, and 2020, respectively; (e–f) scatterplots of daily maximum O_3 with daily maximum NO_2 in DT and non-DT weather in summer of 2018, 2019, and 2020, respectively.

Table 1
Statistical analysis results for the linear regressions in the scatterplots of Fig. 6d–f.

	2018		2019		2020	
	Non-DT	DT	Non-DT	DT	Non-DT	DT
Slope	0.22 ± 0.05	0.36 ± 0.13	0.12 ± 0.06	0.22 ± 0.05	0.21 ± 0.07	0.65 ± 0.20
p value	0.000	0.007	0.067	0.148	0.002	0.003
R^2	0.06	0.18	0.01	0.22	0.04	0.24

Another important compound that can enhance O_3 formation is CO (Jacobson, 2002). CO concentrations had decreased by 41% in Chicago in 2005–2013 in response to emission control efforts (Jing et al., 2014). Results in this study show that CO decreased by 38% from 2015 to 2020 (Fig. 4f). However, CO in 2020 was slightly higher than both 2018 and 2019. This increase cannot be explained by the reduced fossil-fuel burning activities in 2020. We think this increase could have been caused by transported CO from wildfires on the west coast in 2020. This needs further investigation. The added CO could also have contributed to greater O_3 formation in Chicago.

3.3. O_3 and meteorological conditions

The production of ground-level O_3 is affected not only by the emissions of its precursors (i.e., NO_x and VOC), but also by meteorological conditions (i.e., temperature, cloud cover, wind speed/direction). Ozone production is greater on warm, sunny days when the air is stagnant than on days when it is cool, cloudy, and windy (Cox and Chu, 1996; Lee et al., 2012). The SSC method considers all surface weather conditions and provides a more holistic description of daily weather than the individual elements taken separately (Sheridan, 2002). Among the six basic SSC types, dry tropical (DT) weather represents hot, dry, and sunny meteorological conditions, which are all conducive to O_3 formation. Consequently, O_3 concentrations have been found to be highest under DT conditions among the six SSC weather types (Davis et al., 2010; Jing et al., 2016). Although DT weather occurs only 10% of summertime in Chicago, up to 88% of DT days were associated with high O_3 concentrations (>70 ppb) (Jing et al., 2016). Therefore, in addition to analyzing the changes in temperature and precipitation, this study compares the O_3–NO_2 relationship in non-DT weather with that in DT.

In 2015–2020, both the summertime temperature and the number of DT days increased (Fig. 4g and h). The mean air temperature increased by 0.31 ± 0.23 °C/yr ($R^2 = 0.30$), and the number of DT days increased by 1.8 ± 1.2 days/yr ($R^2 = 0.35$). Although NO_x emissions dropped in 2020, the hot, dry weather likely resulted in greater O_3 productivity. It is also shown that Chicago had a cooler summer in 2019, which could have caused O_3 to be lower than in other years, including 2020, if other conditions would have remained constant. There were similar temperatures and numbers of DT days in 2020 as in 2018. Therefore, we next compare 2020 to both 2018 and 2019 to examine the relationship of O_3 with weather conditions. The results show that mean summertime O_3 concentrations in Chicago in 2018–2020 were 18 ppb higher in DT weather than in non-DT weather, and 30–90% of the days with $O_3 > 70$ ppb were associated with DT weather (Fig. 6a–c). The scatter plots (Fig. 6d–f) between daily maximum O_3 and daily maximum NO_2 demonstrate that there was a weak but statistically significant positive correlation between O_3 and NO_2, shown by the positive slope and low R^2 value (Table 1). The positive slope at all NO_2 concentrations suggests that O_3 production is generally NO_x-limited in the Chicago area. In all the three years, O_3 increased more rapidly with NO_2 in DT than in non-DT weather; and the slope of O_3/NO_2 under DT was steepest and most NO_x-limited in 2020 among the three years (Table 1). Taken together, these results suggest that even though NO_x emissions dropped in 2020, the warmer temperatures and greater number of DT days in summer 2020 might have resulted in more efficient production of O_3, which contributed to the O_3 increase in 2020. Furthermore, there was less precipitation in 2020 than in 2018 and 2019, which might have lowered

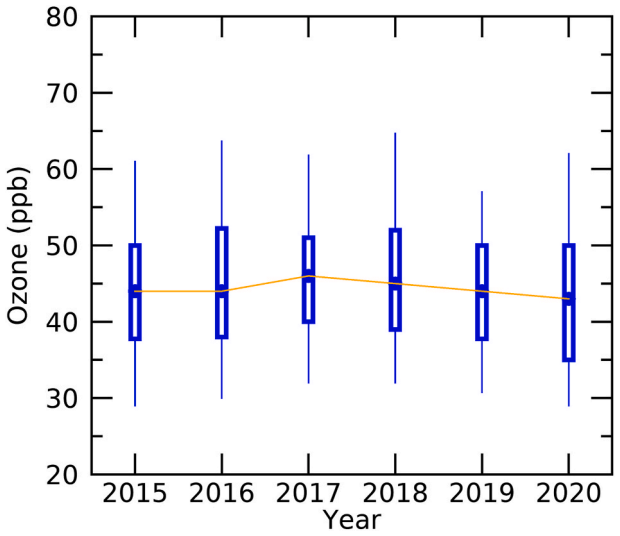

Fig. 7. Summertime O_3 concentration changes at the three rural sites in 2015–2020. Boxes represent the 25th and 75th percentiles, whiskers represent the 5th and 95th percentiles of the considered data (daily maximum O_3 in May–August). The orange line represents the changes of the median values. (For interpretation of the references to colour in this figure legend, the reader is referred to the Web version of this article.)

removal of O_x via the $O(^1D) + H_2O \rightarrow 2OH$ loss pathway (Bates and Jacob, 2019) (Fig. 4i). The mean O_x value, a measure of net photochemical production of O_3, did not increase as dramatically as the O_3 concentration (Fig. 4d), indicating that the elevated O_3 concentrations may be caused by greater physical accumulation of O_3 related to more air stagnation (Figure S2) and lower removal of O_x due to less rainfall (Fig. 4i).

We analyzed the O_3 measurements at the three rural sites that are located west and southwest of Chicago to determine the role of O_3 transported from upwind areas (Fig. 7). The results at the rural sites show that the median O_3 value was 43 ppb in 2020, which was 1–3 ppb lower than the values in 2015–2019; the 5th and 25th percentiles dropped by 1–3 ppb and 2–5 ppb from values in 2015–2019, respectively; the 75th percentile in 2020 was 50 ppb which was the same as the value in 2019 and 1–2 ppb lower than values in 2016–2018; and the 95th percentile in 2020 was 2–3 ppb lower than values in the previous five years except for 2019 which had a cooler summer. The results are consistent with Simon et al. (2015) which reported that summer 5th and 95th percentile O_3 concentrations in rural areas of central U.S. had decreased at about 1 ppb/yr in 1998–2013. All the results indicate that background O_3 levels were lower in 2020 than in the previous five years. Therefore, the slight increase of O_3 in Chicago in 2020 (Fig. 4a) was unlikely to be caused by the transport of background O_3. It is also possible that transport of O_3 precursors, NO_x and VOCs, from upwind areas may affect O_3 in Chicago. The time scale of DT weather is synoptic (typically days), whereas the lifetimes of surface NO_x and VOCs are hours. Therefore, the impact of DT weather on O_3 is mostly the result of changed meteorological conditions for O_3 production and accumulation (hotter temperature, lower humidity, and less ventilation).

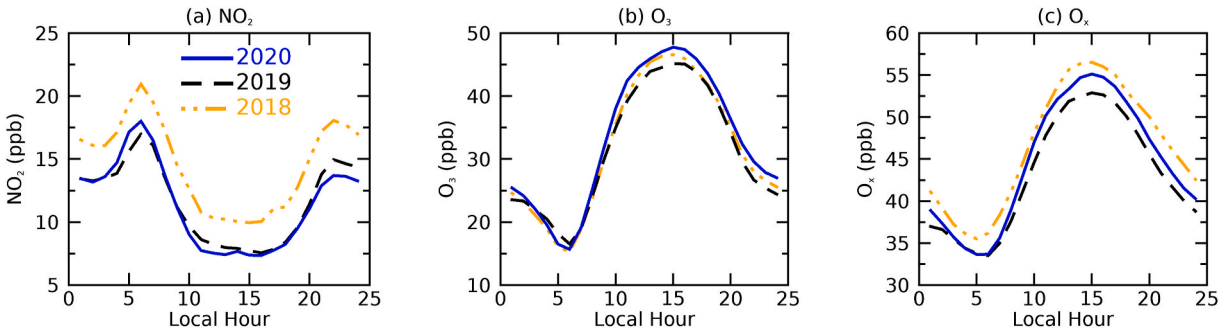

Fig. 8. (a–c) Average summertime hourly mixing ratios of NO_2, O_3, and O_x, respectively, in 2018, 2019, and 2020 at the three AQS sites in Chicago that measure both NO_2 and O_3.

3.4. Diurnal cycles of O_3, NO_2, and O_x

To explain why O_3 concentration was highest in 2020 among 2018, 2019, and 2020, and to resolve discrepancies in NO_2 between TROPOMI and ground monitors, we examined the diurnal cycles of NO_2, O_3, and O_x using their hourly concentrations (Fig. 8a–c). Diurnal cycles can better reflect changes in local photochemistry. The shapes of the NO_2 and O_3 diurnal cycles were similar among 2018, 2019, and 2020 (Fig. 8a and b). NO_2 concentrations peak around 6:00 due to the stagnant winds, low boundary layer height, and emissions from morning commuter traffic. The available sunlight after 6:00 results in the photolysis of NO_2 and photochemical formation of O_3. Consequently, NO_2 drops rapidly and O_3 increases rapidly after 6:00 until 15:00 when NO_2 is the lowest and O_3 concentration peaks. After 15:00, O_3 decreases throughout the night until 6:00 the following day due to reduced photochemical formation and net destruction of O_3. The diurnal cycle of O_x shows that the net formation of O_3 peaks around 15:00 and reaches its lowest level at 6:00 (Fig. 8c). NO_2 increases between 15:00 and 22:00 because of increased emissions from commuter traffic and reduced photolysis of NO_2 due to lack of sunlight. NO_2 decreases again between 22:00 and 3:00 the next day because of reduced NO_x emissions. Interestingly, NO_2 concentrations were higher in 2020 than 2019 in the early morning (3:00–7:00), but lower in 2020 than 2019 at mid-day (10:00–15:00), which is consistent with the satellite measurements.

The differences shown in the diurnal cycles of NO_2 and O_3 among the three years indicate differences in the NO_x-O_3 photochemistry (Fig. 8a and b). First, the hourly NO_2 concentrations were highest in 2018, followed by 2019, and lowest in 2020, consistent with NO_x emissions being highest in 2018 and lowest in 2020. Between 1:00 and 6:00, NO_2 in 2020 was higher than in 2019. This might have been caused by nighttime meteorological conditions (such as reduced boundary layer height and increased air stagnation). Second, the hourly O_x values were highest in 2018, consistent with the highest NO_x emissions in 2018 (Fig. 8c). However, hourly O_x was higher in 2020 than in 2019, indicating that the net production of O_3 was higher in 2020 while NO_x emissions were lower. With even lower NO_x emissions in 2020, greater amounts of O_3 were still produced due to increases in temperature, CO concentrations, and HCHO concentrations (Fig. 4g–i). It is uncertain why the CO and HCHO concentrations increased in 2020 from 2019. It could be because the warmer temperatures resulted in greater biogenic emissions of VOC, which oxidize to HCHO and CO. Another contribution could be the transported CO and VOCs from wildfires on the west coast of the U.S. in 2020, but further investigation is needed.

4. Conclusion and discussion

The COVID-19 lockdowns resulted in reduced NO_x emissions. According to TROPOMI measurements, the mean 2020 summertime tropospheric NO_2 in Chicago dropped by 18% from the previous two years. However, O_3 in Chicago did not show a decrease in 2020 corresponding to the reduced NO_x emissions, although O_3 at the rural sites upwind of Chicago decreased. Our results also show that there was more-efficient O_3 production from NO_2 in 2020, and it was correlated with the hot, dry weather condition. In 2015–2020, the two years that had the lowest number of $O_3 > 70$ ppb days were 2015 and 2019, which also had the lowest number of DT weather days. This indicates the relative importance of weather conditions in the occurrence of high-O_3 episodes in Chicago. The fact that even the lockdowns did not cause O_3 in Chicago to decrease indicates that we need to pay attention to the potential future impacts of climate change on air pollution in Chicago, as studies have shown that hot, dry, and stagnant weather conditions are likely to occur more frequently in the future (Mickley et al., 2004; Horton et al., 2014). Climate change can also aggravate O_3 pollution by producing more frequent and more severe wildfires, and fire emissions could enhance O_3 formation (Jaffe and Wigder, 2012; Zhang and Wang, 2016; Lin et al., 2017). Focusing on NO_x emission reductions regionwide and VOC emission reductions within the city will be necessary to overcome the increasingly conducive weather for ozone formation and safeguard human health.

Credit author statement

Ping Jing: Funding acquisition, Conceptualization, Methodology, Formal analysis, Visualization & Writing – original draft. Daniel L. Goldberg: Methodology, Formal analysis, Visualization & Writing – review & editing.

Declaration of competing interest

The authors declare that they have no known competing financial interests or personal relationships that could have appeared to influence the work reported in this paper.

Acknowledgments

This work is supported by the Loyola University Chicago 2021 Summer Research Stipends. The ozone-related air quality data are obtained from the Air Data archives of the U.S. Environmental Protection Agency (https://www.epa.gov/outdoor-air-quality-data); the observed daily air temperature and precipitation data are provided by the Midwestern Regional Climate Center (https://mrcc.illinois.edu/CLIMATE/); the daily synoptic weather types are obtained from the Spatial Synoptic Classification (http://sheridan.geog.kent.edu/ssc.html); the monthly-mean tropospheric column ozone data are provided by the National Aeronautics and Space Administration's Goddard Space Flight Center (https://acd-ext.gsfc.nasa.gov/Data_services/cloud_slice/new_data.html).

Appendix A. Supplementary data

Supplementary data to this article can be found online at https://doi.org/10.1016/j.apr.2021.101313.

References

American Lung Association, 2019. State of the Air 2019. Retrieved from. https://www.lung.org/assets/documents/healthy-air/state-of-the-air/sota-2019-full.pdf.

Bates, K.H., Jacob, D.J., 2019. A new model mechanism for atmospheric oxidation of isoprene: global effects on oxidants, nitrogen oxides, organic products, and secondary organic aerosol. Atmos. Chem. Phys. 19, 9613–9640.

Bauwens, M., Compernolle, S., Stavrakou, T., Müller, J.-F., van Gent, J., Eskes, H., Levelt, P.F., der Van, A.R., Veefkind, J.P., Vlietinck, J., Yu, H., Zehner, C., 2020. Impact of coronavirus outbreak on NO_2 pollution assessed using TROPOMI and OMI observations. Geophys. Res. Lett. 47, e2020GL087978.

Bloomer, B.J., Stehr, J.W., Piety, C.A., Salawitch, R.J., Dickerson, R.R., 2009. Observed relationships of ozone air pollution with temperature and emissions. Geophys. Res. Lett. 36, L09803. https://doi.org/10.1029/2009GL037308.

Brancher, M., 2021. Increased ozone pollution alongside reduced nitrogen dioxide concentrations during Vienna's first COVID-19 lockdown: significance for air quality management. Environ. Pollut. 284, 117153.

Camalier, L., Cox, W., Dolwick, P., 2007. The effects of meteorology on ozone in urban areas and their use in assessing ozone trends. Atmos. Environ. 41, 7127–7137.

Cazorla, M., Herrera, E., Palomeque, E., Saud, N., 2021. What the COVID-19 lockdown revealed about photochemistry and ozone production in Quito, Ecuador. Atmos. Pollut. Res. 12, 124–133.

Cox, W.M., Chu, S.-H., 1996. Assessment of interannual ozone variation in urban areas from a climatological perspective. Atmos. Environ. 30, 2615–2625.

Davis, R.E., Normile, C.P., Sitka, L., Hondula, D.M., Knight, D.B., Gawtry, S.P., Stenger, P.J., 2010. A comparison of trajectory and air mass approaches to examine ozone variability. Atmos. Environ. 44, 64–74.

De Smedt, I., Stavrakou, T., Hendrick, F., Danckaert, T., Vlemmix, T., Pinardi, G., Theys, N., Lerot, C., Gielen, C., Vigouroux, C., Hermans, C., Fayt, C., Veefkind, P., Muller, J.F., Van Roozendael, M., 2015. Diurnal, seasonal, and long-term variations of global formaldehyde columns inferred from combined OMI and GOME-2 observations. Atmos. Chem. Phys. 15 https://doi.org/10.5194/acp-15-12519-2015, 12519e12545.

Duncan, B.N., Yoshida, Y., Olson, J.R., Sillman, S., Martin, R.V., Lamsal, L., Hu, Y., Pickering, K.E., Retscher, C., Allen, D.J., Crawford, J.H., 2010. Application of OMI observations to a space-based indicator of NO_x and VOC controls on surface ozone formation. Atmos. Environ. 44, 2213–2223.

Forster, P.M., Forster, H.I., Evans, M.J., Gidden, M.J., Jones, C.D., Keller, C.A., Lamboll, R.D., Le Quéré, C., Rogelj, J., Rosen, D., Schleussner, C.F., 2020. Current and future global climate impacts resulting from COVID-19. Nat. Clim. Change 10, 913–919.

Gaubert, B., Bouarar, I., Doumbia, T., Liu, Y., Stavrakou, T., Deroubaix, A., Darras, S., Elguindi, N., Granier, C., Lacey, F., Müller, J.F., 2021. Global changes in secondary atmospheric pollutants during the 2020 COVID-19 pandemic. J. Geophys. Res. 126, e2020JD034213.

Goldberg, D.L., Anenberg, S.C., Griffin, D., McLinden, C.A., Lu, Z., Streets, D.G., 2020. Disentangling the impact of the COVID-19 lockdowns on urban NO_2 from natural variability. Geophys. Res. Lett. 47, e2020GL089269.

Guenther, A., Karl, T., Harley, P., Wiedinmyer, C., Palmer, P.I., Geron, C., 2006. Estimates of global terrestrial isoprene emissions using MEGAN (model of emissions of gases and aerosols from nature). Atmos. Chem. Phys. 6, 3181–3210.

Harkins, C., McDonald, B.C., Henze, D.K., Wiedinmyer, C., 2021. A fuel-based method for updating mobile source emissions during the COVID-19 pandemic. Environ. Res. Lett. 16, 65018.

He, C., Hong, S., Zhang, L., Mu, H., Xin, A., Zhou, Y., Yang, L., 2021. Global, continental, and national variation in $PM_{2.5}$, O_3, and NO_2 concentrations during the early 2020 COVID-19 lockdown. Atmospheric Pollut. Ress 12, 136–145.

Horton, D.E., Skinner, C.B., Singh, D., Diffenbaugh, N.S., 2014. Occurrence and persistence of future atmospheric stagnation events. Nat. Clim. Change 4, 698–703.

Jacob, D.J., 1999. Introduction to Atmospheric Chemistry. Princeton University Press.

Jacobson, M.Z., 2002. Atmospheric Pollution: History, Science, and Regulation. Cambridge University Press.

Jaffe, D.A., Wigder, N.L., 2012. Ozone production from wildfires: a critical review. Atmos. Environ. 51, 1–10.

Jaffe, D.A., Zhang, L., 2017. Meteorological anomalies lead to elevated O_3 in the western U.S. in June 2015. Geophys. Res. Lett. 44 https://doi.org/10.1002/2016GL072010.

Jin, X., Fiore, A.M., Murray, L.T., Valin, L.C., Lamsal, L.N., Duncan, B., Folkert Boersma, K., De Smedt, I., Abad, G.G., Chance, K., Tonnesen, G.S., 2017. Evaluating a space-based indicator of surface ozone-NO_x-VOC sensitivity over mid-latitude source regions and application to decadal trends. J. Geophys. Res. 122 https://doi.org/10.1002/2017JD026720.

Jin, X., Fiore, A., Boersma, K.F., De Smedt, I., Valin, L., 2020. Inferring changes in summertime surface ozone–NO_x–VOC chemistry over US urban areas from two decades of satellite and ground-based observations. Environ. Sci. Technol. 54, 6518–6529.

Jing, P., Lu, Z., Xing, J., Streets, D.G., Tan, Q., O'Brien, T., Kamberos, J., 2014. Response of the summertime ground-level ozone trend in the Chicago area to emission controls and temperature changes, 2005–2013. Atmos. Environ. 99, 630–640.

Jing, P., O'Brien, T., Streets, D.G., Patel, M., 2016. Relationship of ground-level ozone with weather patterns in Chicago. Urban Clim. 17, 161–175.

Jing, P., Lu, Z., Steiner, A.L., 2017. The ozone climate penalty in the Midwestern. U.S. Atmos. Environ. 170, 130–142.

Kerr, G.H., Waugh, D.W., Strode, S.A., Steenrod, S.D., Oman, L.D., Strahan, S.E., 2019. Disentangling the drivers of the summertime ozone-temperature relationship over the United States. J. Geophys. Res. Atmos. https://doi.org/10.1029/2019JD030572.

Lee, C.C., Ballinger, T.J., Domino, N.A., 2012. Utilizing map pattern classification and surface weather typing to relate climate to the air quality index in Cleveland, Ohio. Atmos. Environ. 63, 50–59.

Lin, M., Horowitz, L.W., Payton, R., Fiore, A.M., Tonnesen, G., 2017. US surface ozone trends and extremes from 1980 to 2014: quantifying the roles of rising Asian emissions, domestic controls, wildfires, and climate. Atmos. Chem. Phys. 17, 2943–2970.

Martin, R.V., Fiore, A.M., Van Donkelaar, A., 2004. Space-based diagnosis of surface ozone sensitivity to anthropogenic emissions. Geophys. Res. Lett. 31 https://doi.org/10.1029/2004GL019416.

McDonald, B.C., de Gouw, J.A., Gilman, J.B., Jathar, S.H., Akherati, A., Cappa, C.D., Jimenez, J.L., Lee-Taylor, J., Hayes, P.L., McKeen, S.A., Cui, Y.Y., 2018. Volatile chemical products emerging as largest petrochemical source of urban organic emissions. Science 359, 760–764.

Mickley, L.J., Jacob, D.J., Field, B.D., Rind, D., 2004. Effects of future climate change on regional air pollution episodes in the United States. Geophys. Res. Lett. 31, L24103. https://doi.org/10.1029/2004GL021216.

Miyazaki, K., Bowman, K., Sekiya, T., Takigawa, M., Neu, J.L., Sudo, K., Osterman, G., Eskes, H., 2021. Global tropospheric ozone responses to reduced NOx emissions linked to the COVID-19 worldwide lockdowns. Sci. Adv. 7, eabf7460.

Naqvi, H.R., Mutreja, G., Hashim, M., Singh, A., Nawazuzzoha, M., Naqvi, D.F., et al., 2021. Global assessment of tropospheric and ground air pollutants and its correlation with COVID-19. Atmos. Pollut. Res. 12, 101172.

Schroeder, J.R., Crawford, J.H., Fried, A., Walega, J., Weinheimer, A., Wisthaler, A., Müller, M., Mikoviny, T., Chen, G., Shook, M., Blake, D.R., Tonnesen, G.S., 2017. New insights into the column CH_2O/NO_2 ratios as an indicator of near-surface ozone sensitivity. J. Geophys. Res. 122, 8885–8907. https://doi.org/10.1002/2017JD026781.

Sheridan, S.C., 2002. The redevelopment of a weather-type classification scheme for North America. Int. J. Climatol. 22, 51–68.

Sillman, S., 1995. The use of NO_y, H_2O_2, and HNO_3 as indicators for ozone-NO_x-hydrocarbon sensitivity in urban locations. J. Geophys. Res. 100, 14175–14188.

Simon, H., Reff, A., Wells, B., Xing, J., Frank, N., 2015. Ozone trends across the United States over a period of decreasing NOx and VOC emissions. Environ. Sci. Technol. 49, 186–195. https://doi.org/10.1021/es504514z.

Sokhi, R.S., Singh, V., Querol, X., Finardi, S., Targino, A.C., de Fatima Andrade, M., et al., 2021. A global observational analysis to understand changes in air quality during exceptionally low anthropogenic emission conditions. Environ. Int. 157, 106818.

Soni, M., Ojha, N., Girach, I., 2021. Impact of COVID-19 lockdown on surface ozone build-up at an urban site in western India based on photochemical box modelling. Curr. Sci. 120, 376.

Steinbrecht, W., Kubistin, D., Plass-Dülmer, C., Davies, J., Tarasick, D.W., Gathen, P.V.D., Deckelmann, H., Jepsen, N., Kivi, R., Lyall, N., Palm, M., 2021. COVID-19 crisis reduces free tropospheric ozone across the Northern Hemisphere. Geophys. Res. Lett. 48, e2020GL091987.

Sun, W., Zhu, L., De Smedt, I., Bai, B., Pu, D., Chen, Y., Shu, L., Wang, D., Fu, T.M., Wang, X., Yang, X., 2021. Global significant changes in formaldehyde (HCHO) columns observed from space at the early stage of the COVID-19 pandemic. Geophys. Res. Lett. 48, 2e020GL091265.

U.S. Environmental Protection Agency, 2021. Green Book. Retrieved from. https://www.epa.gov/green-book.

Wilson, J.G., Kingham, S., Pierce, J., Struman, A.P., 2005. A review of intraurban variations in particulate air pollution: implications for epidemiological research. Atmos. Environ. 39, 6444–6462.

Yadav, V., Turner, J., 2014. Gauging intraurban variability of ambient particulate matter arsenic and other air toxic metals from a network of monitoring sites. Atmos. Environ. 89, 318–328.

Zhang, Y., Wang, Y., 2016. Climate-driven ground-level ozone extreme in the fall over the Southeast United States. Proc. Natl. Acad. Sci. Unit. States Am. 113, 10025–10030. https://doi.org/10.1073/pnas.1602563113.

Zhu, L., Jacob, D.J., Mickley, L.J., Marais1, E.A., Cohan, D.S., Yoshida, Y., Duncan, B.N., Abad, G.G., Chance, K.V., 2014. Anthropogenic emissions of highly reactive volatile organic compounds in eastern Texas inferred from oversampling of satellite (OMI) measurements of HCHO columns. Environ. Res. Lett. 9 https://doi.org/10.1088/1748-9326/9/11/114004.

Ziemke, J.R., Chandra, S., Duncan, B.N., Froidevaux, L., Bhartia, P.K., Levelt, P.F., Waters, J.W., 2006. Tropospheric ozone determined from aura OMI and MLS: evaluation of measurements and comparison with the global modeling initiative's chemical transport model. J. Geophys. Res. 111, D19303.